LBNL-44607
hep-ph/9911443

Anomalous Higgs-Photon Interactions in Photon Fusion Processes at NLC

S. M. Lietti
Theory Group, Lawrence Berkeley National Laboratory,
Berkeley, CA 94530, USA.
(November 24, 1999)

Abstract

The Standard Model (SM) of the electroweak has proven to be successful in describing all the available precision experimental data. However, the Higgs mechanism, responsible for the electroweak symmetry breaking in the SM, still remains one of the most important open questions of the theory. The effect of new operators that give rise to anomalous Higgs boson coupling to two photons is examined in the two-photon processes $\gamma\gamma \to H \to b\bar{b}, \gamma\gamma, W^+W^-, ZZ$ at a high energy linear e^+e^- collider (NLC).

I. INTRODUCTION

The Standard Model (SM) of the electroweak interactions based on the gauge group $SU(2)_L \times U(1)_Y$ has proven to be successful in describing all the available precision experimental data [1]. This applies particularly to the predictions for the couplings of the gauge bosons to the matter fermions. The recent measurements of the gauge-boson self couplings at LEPII [2] and Tevatron [3] collider also shed some light on the correctness of the SM predictions for these interactions.

On the other hand, the precise mechanism of the electroweak symmetry breaking still remains one of the most important open questions of the theory. In the SM, the breaking is realized via the Higgs mechanism in which a scalar $SU(2)$-doublet, the Higgs boson, is introduced *ad hoc* and the symmetry is spontaneously broken by the vacuum expectation value (VEV) of the Higgs field. However, in this simple realization, the theory presents problems since the running Higgs mass shows a quadratic divergence at some high scale. This may imply the existence of a cut-off scale Λ above which new physics must appear.

The experiments which will take place at the Next Linear electron–positron Collider (NLC) will be able to explore the nature of the Higgs boson and its couplings to other particles [4]. Deviations from the SM predictions for these couplings would indicate the existence of new physics effects.

In general, such deviations can be parametrized in terms of effective Lagrangians by adding to the SM Lagrangian higher dimensional operators that describe the new phenomena [5]. This model–independent approach accounts for new physics that shows up at an energy scale Λ, larger than the electroweak scale. The effective Lagrangians are constructed with the light particle spectrum that exists at low energies, while the heavy degrees of freedom are integrated out. They are invariant under the $SU(2)_L \times U(1)_Y$ and, in the linearly realized version, they involve, in addition to the usual gauge–boson fields, also the light Higgs particle. The most general dimension–6 effective Lagrangian, containing all SM bosonic fields, that is C and P even, was constructed in Ref. [6].

Out of the eleven independent operators constructed in Ref. [6], three of them describe new interaction between the Higgs particle and the photon,

$$\mathcal{L}_{\rm eff} = \frac{f_{WW}}{\Lambda^2}\,\Phi^\dagger \hat{W}_{\mu\nu}\hat{W}^{\mu\nu}\Phi + \frac{f_{BB}}{\Lambda^2}\,\Phi^\dagger \hat{B}_{\mu\nu}\hat{B}^{\mu\nu}\Phi + \frac{f_{BW}}{\Lambda^2}\,\Phi^\dagger \hat{B}_{\mu\nu}\hat{W}^{\mu\nu}\Phi\;, \tag{1}$$

where, in the unitary gauge, the Higgs doublet becomes $\Phi = (1/\sqrt{2})[\,0\,,\,(v+H)\,]^T$, $\hat{B}_{\mu\nu} = i(g'/2)B_{\mu\nu}$, and $\hat{W}_{\mu\nu} = i(g/2)\sigma^a W^a_{\mu\nu}$, with $B_{\mu\nu}$ and $W^a_{\mu\nu}$ being the field strength tensors of the $U(1)$ and $SU(2)$ gauge fields respectively, and Λ represents the energy scale for new physics.

The operators of Eq. (1) describe the effect, at one–loop level [7], of new heavy states predicted by the underlying theory that should be valid at very high energies. The possible existence of heavy fermions and/or bosons, that couple to the (light) bosonic sector of the SM, should indirectly manifest itself in the Higgs boson couplings via equation (1), after all the heavy degrees of freedom are integrated out. Anomalous Higgs boson couplings have already been studied in Higgs and Z boson decays [8], in e^+e^- [9–11], $\gamma\gamma$ [12], and $p\bar{p}$ colliders [13].

In this paper, we explore the consequence of new operators that give rise to an anomalous Higgs boson coupling to photons ($H\gamma\gamma$). In particular, we study the anomalous production of

the Higgs boson via two-photon processes in a electron-positron collider, with the subsequent decay of the Higgs boson into two particles. It is important to notice that we have also taken into account the SM one–loop Higgs contributions [14,15] to this vertex in our analyses.

The lagrangian in Eq. (1) induces, besides the $H\gamma\gamma$ coupling, other anomalous Higgs couplings like $HZ\gamma$, HZZ, and HW^+W^-. In the unitary gauge, Eq. (1) can be written for the anomalous Higgs couplings as,

$$\mathcal{L}_{\rm eff}^{\rm H} = g_{H\gamma\gamma} H A_{\mu\nu} A^{\mu\nu} + g_{HZ\gamma} H A_{\mu\nu} Z^{\mu\nu} + g_{HZZ} H Z_{\mu\nu} Z^{\mu\nu} + g_{HWW} H W^+_{\mu\nu} W^{\mu\nu}_- \quad , \tag{2}$$

where $A_{\mu\nu} = \partial_\mu A_\nu - \partial_\nu A_\mu$ and the same for $Z_{\mu\nu}$. The effective couplings $g_{H\gamma\gamma}$, $g_{HZ\gamma}$, g_{HZZ}, and g_{HWW} are related to the coefficients of the operators appearing in Eq. (1). In particular, for the $H\gamma\gamma$ coupling one has,

$$g_{H\gamma\gamma} = -\frac{g m_W \sin^2\theta_W}{2} \left(\frac{f_{BB} + f_{WW} - f_{BW}}{\Lambda^2} \right) \quad . \tag{3}$$

Considering only the effect of one operator at a time and combining information from precision measurements at LEPI and at low energy, one has the following constraints at 95% CL (in units of TeV^{-2}) [16], for $m_H = 200$ GeV and $m_{\rm top} = 175$ GeV,

$$-1. \leq \frac{f_{BW}}{\Lambda^2} \leq 8.6 \quad , \quad -79 \leq \frac{f_{BB}}{\Lambda^2} \leq 47 \quad , \quad -24 \leq \frac{f_{WW}}{\Lambda^2} \leq 14 \quad . \tag{4}$$

Anomalous Higgs boson production via vector boson fusion can be also generated by the anomalous couplings $HZ\gamma$ – HW^+W^- and HZZ of Eq. (2) are not considered here since their effect is much less important than the anomalous Higgs boson production via two-photon process due to phase space reduction.

In order to impose limits on the dimension–6 operators of Eq. (1) which generate the new $H\gamma\gamma$ interaction, we examine the Higgs boson production via two-photon process at the NLC with the subsequent decay into $\gamma\gamma$, $b\bar{b}$, W^+W^-, ZZ. The SM background considered for these reactions can be divided in two groups:

- Set I: all the SM direct contribution for $e^+e^- \to \gamma\gamma$, $b\bar{b}$, W^+W^-, and ZZ;
- Set II: the vector boson fusion contributions $e^+e^- \to W^+W^-(\nu\bar{\nu}) \to \gamma\gamma(\nu\bar{\nu})$, $b\bar{b}(\nu\bar{\nu})$, $W^+W^-(\nu\bar{\nu})$, $ZZ(\nu\bar{\nu})$, and $e^+e^- \to ZZ(e^+e^-) \to \gamma\gamma(e^+e^-)$, $b\bar{b}(e^+e^-)$, $W^+W^-(e^+e^-)$, $ZZ(e^+e^-)$.

II. VECTOR BOSON FUSION AT NLC

In the case of a high energy electron-positron collider, virtual gauge bosons can be produced nearly on–shell and collinear with the initial particles. If one uses the effective boson approximation [17,18] one may regard the fermion beams as sources of gauge bosons and at leading log ignore the virtuality of these bosons in calculating the cross section. The process $f_a + f_b \to f_{a'} + f_{b'} + X$, where both f_a and f_b serve as source of a vector boson, can be evaluated by the effective boson approximation formula [18]

$$\sigma_{f_a+f_b\to f_{a'}+f_{b'}+X}(s_0) = \int dx_1 \int dx_2 f_n(x_1) f_m(x_2) \hat{\sigma}^{nm}_{V_1+V_2\to f_{a'}+f_{b'}+X}(\hat{s}_0) \tag{5}$$

where $\hat{s}_0 = x_1 x_2 s_0$, $V_{1,2} = W^{\pm}$ or Z^0, and $m, n = -1, 0, 1$ are the vector boson helicities. If one writes the elementary coupling between the fermions and the vector boson as $\bar{\Psi}\Gamma_\mu \Psi V^\mu$ with

$$\Gamma_\mu = g_R \frac{\gamma_\mu(1+\gamma_5)}{2} + g_L \frac{\gamma_\mu(1-\gamma_5)}{2},$$

one obtains the following distribution function:

$$\begin{aligned} f_{-1} &= g_R^2 h_1 + g_L^2 h_2, \\ f_0 &= (g_L^2 + g_R^2) h_0, \\ f_1 &= g_L^2 h_1 + g_R^2 h_2, \end{aligned}$$

where

$$\begin{aligned} h_0 &= \left[\frac{x}{16\pi^2}\right]\left[\frac{2(1-x)\xi}{w^2 x} - \frac{2\Delta(2-w)}{w^3}\log\left(\frac{x}{\Delta'}\right)\right], \\ h_1 &= \left[\frac{x}{16\pi^2}\right]\left[\frac{-(1-x)(2-w)}{w^2} + \frac{(1-w)(\xi-w^2)}{w^3}\log\left(\frac{1}{\Delta'}\right) - \frac{\xi-2xw}{w^3}\log\left(\frac{1}{x}\right)\right], \\ h_2 &= \left[\frac{x}{16\pi^2}\right]\left[\frac{-(1-x)(2-w)}{w^2(1-w)} + \frac{\xi}{w^3}\log\left(\frac{x}{\Delta'}\right)\right], \end{aligned}$$

where $w = x - \Delta$, $\xi = x + \Delta$, $\Delta = M_V^2/s^0$, and $\Delta' = \Delta/(1-w)$.

This approach will be used to evaluate the vector boson fusion background (Set II) described in Section I.

III. ANOMALOUS HIGGS BOSON PRODUCTION VIA TWO-PHOTON PROCESS AT NLC

For a high energy electron-positron collider, two-photon processes can be calculated using an effective photon approximation [19] so that if a cross section $\sigma_{\gamma\gamma\to X}$ is known, the cross section for $e^+e^- \to e^+e^-X$ via the two photon mechanism is given by:

$$\sigma_{e^+e^-\to e^+e^-X}(s_0) = \left[\frac{\alpha}{2\pi}\log\left(\frac{s_0}{4\hat{m}_e^2}\right)\right]^2 \int_0^1 f(\tau)\sigma_{\gamma\gamma\to X}(\tau s_0)d\tau, \tag{6}$$

where s_0 is the square of the center of mass energy of the initial e^+e^- and

$$f(\tau) = \frac{1}{\tau}[(2+\tau)^2 \log\frac{1}{\tau} - 2(1-\tau)(3+\tau)]. \tag{7}$$

In this expression the total cross section for $e^+e^- \to e^+e^-X$ is given if one takes $\hat{m}_e = m_e = 0.5$ MeV as the mass of the electron. However, if one wishes to observe the e^+e^- in the final state, experimental constrains require that a minimum cut on the transverse momentum of the final state electron $P_{T_{min}}$ be used. In this case the result is given by taking $\hat{m}_e = P_{T_{min}}$.

In order to study the anomalous Higgs boson production via two-photon process at NLC we do not necessarily need to observe the final e^+e^- pair because it is not a product

of the Higgs boson decay. Besides, for a NLC with $\sqrt{s_0} = 500(1000)$ GeV and requiring $P_{T_{min}} = 20(40)$ GeV one finds that the cross section of Eq. (6) is only 3.7(3.3)% of the total cross section for $\hat{m}_e = m_e = 0.5$ MeV. Therefore, more than 96 % of the anomalous Higgs boson production via photon fusion happens when the final e^+e^- pair is undetected.

The anomalous contributions for the $H\gamma\gamma$ interaction are significant only when the Higgs boson is produced on–mass–shell, as we will see in section IV. For this reason, we will use the production of $b\bar{b}$ and $\gamma\gamma$ pairs to study a light Higgs boson mass range of $100 \leq m_H \leq 150$ GeV at a NLC with energy $\sqrt{s_0} = 500$ GeV and integrated luminosity $\mathcal{L} = 50$ fb^{-1}. The production of W^+W^- and ZZ pairs will be used to study a heavier Higgs boson mass range of $200 \leq m_H \leq 350$ GeV at a NLC with energy $\sqrt{s_0} = 1$ TeV and integrated luminosity $\mathcal{L} = 100$ fb^{-1}. We have considered in our analyses a 80% detection efficiency for each photon and quark bottom, and a 80% overall detection efficiency for the W^+W^- and ZZ final state.

IV. RESULTS

In order to compute the contributions for the signal of anomalous Higgs boson production via photon fusion with subsequent decay into pairs of bottom quarks, photons, and massive gauge bosons W and Z, as well as for the background for these final state pairs of particles via direct, photon, and vector boson fusion production, we have have incorporated all anomalous couplings in Helas–type [20] Fortran subroutines. These new subroutines were used to adapt a Madgraph [21] output to include all the anomalous contributions. We have checked that our code passed the non–trivial test of electromagnetic gauge invariance. We employed Vegas [22] to perform the Monte Carlo phase space integration to obtain the differential and total cross sections for the signal and the background (Sets I and II).

To estimate the impact of the anomalous coefficients f_{BB}, f_{WW}, and f_{BW} in the Higgs boson production via photon fusion, we have evaluated the total cross section for signal and background for all processes described in Section (I). The signal was obtained considering that all anomalous operators coefficients have the same value $f_{all} = f_{BB} = f_{BW} = f_{WW} = 30$ TeV^{-2}, which is in agreement with the limits of Eq.(4). In order to avoid infrared divergences in the two photons final state, we have required these photons to have a transverse momentum of $p_{T_\gamma} \geq 25$ GeV. An analysis of the significance of the signal (Significance = Signal/$\sqrt{\text{Background}}$) shows that the $b\bar{b}$ production is a better option compared to the $\gamma\gamma$ production in order to impose limits on the anomalous coefficients for a light Higgs mass ($100 \leq M_H(GeV) \leq 150$) as one can see in Tables I and II. For higher masses ($200 \leq M_H(GeV) \leq 350$), Tables III and IV show that the W^+W^- production is a better option compared to the ZZ production.

In order to improve the sensitivity of NLC to the anomalous Higgs boson production, we have investigated different distributions of the final state particles for both signal ($f_{all} = 30$ TeV^{-2}) and background. One of most promising variables is the transverse momentum of the final particles whose distribution is presented in Fig. 1 (a) for the $b\bar{b}$ final state and in Fig. 2 (a) for the W^+W^- final state. In both cases, we observe that the contribution of the anomalous Higgs production reaches its maximum contribution in

$$p_{T_{ano}} = \frac{1}{2}\sqrt{M_H^2 - M_{pair}^2}, \tag{8}$$

where M_H is the mass of the Higgs boson and M_{pair} is the sum of the masses of the final particles that should be a product of the Higgs boson decay. Similar behaviour is observed for the $\gamma\gamma$ and ZZ final states. Therefore, we require the transverse momentum of these final state particles to be in the range

$$25 < p_T(\text{GeV}) < (p_{T_{ano}} + 5) \ . \tag{9}$$

In this way, the significance of the signal is enhanced by a factor of at least 1.75, compared to the previous analyses without any cut, as we can see in Tables I-IV. The 95% CL allowed values for the coefficients f_{BB}, f_{WW}, f_{BW}, and f_{all} using the cut (9) are shown in Figures 3 and 4 (dashed lines) for all the final pair productions.

Another promising variable is the invariant mass of the particles produced in the Higgs decay, presented in Fig. 1 (b) for the $b\bar{b}$ final state and Fig. 2 (b) for the W^+W^- final state. Since the contribution of the anomalous couplings is dominated by on–mass–shell Higgs production with the subsequent $H \to b\bar{b}, \gamma\gamma, W^+W^-, ZZ$ decays, as can be clearly seen in the Figures 1 (b) and 2 (b), a more drastic cut would be to require

$$(M_H - 5) < M^{inv}_{pair}(\text{GeV}) < (M_H + 5) \ , \tag{10}$$

where M^{inv}_{pair} is the invariant mass of the final $b\bar{b}$, $\gamma\gamma$, W^+W^-, or ZZ pairs. The best constraints are obtained at NLC when this cut is applied, as we can be seen through the enhancement of the significance in Tables I-IV. The 95%CL results obtained using the cut (10) are also shown in Figures 3 and 4. These results are more restrictive than the constraints obtained at LEPI and at low energy [Eq. (4)] and for $ZZ\gamma$ and $Z\gamma\gamma$ production at LEPII and NLC [11], especially for f_{BB} and f_{WW}.

V. CONCLUSIONS

The search for the effect of higher dimensional operators that give rise to anomalous Higgs boson couplings may provide important information on physics beyond the SM and should be pursued in all possible reactions. In this paper, we have studied the $b\bar{b}$, $\gamma\gamma$, W^+W^-,and ZZ production in high energy e^+e^- colliders (NLC) via photon fusion, focusing on the operators that generate anomalous $H\gamma\gamma$ coupling.

We established the limits that can be imposed at NLC through the analysis of the impact of the anomalous coupling over the total cross section of processes involving two final bottons, photons, W's, and Z's bosons. In order to improve the sensitivity of NLC to this anomalous Higgs boson production, the limits were evaluated for the cases where a convenient cut on the transverse momentum spectrum and on the invariant mass spectrum of the final state particles is used.

Typical values of a few TeV^{-2} are reached in our analyses. Our results are more restrictive than the constraints obtained at low energy data, at LEPI, and for $ZZ\gamma$ and $Z\gamma\gamma$ production at LEPII and NLC [11]. Therefore, the NLC should provide important hints about the existence of new physics beyond the Standard Model.

ACKNOWLEDGMENTS

I would like to thank S.F. Novaes and J.K. Mizukoshi for very useful discussions. This work was supported in part by the Director, Office of Science, Office of Science, Office of Basic Energy Services, of the U.S. Department of Energy under Contract DE-AC03-76SF00098 and in part by Fundação de Amparo à Pesquisa do Estado de São Paulo (FAPESP).

REFERENCES

[1] See, for instance: G. Altarelli, preprint CERN-TH.97-278, and e-Print Archive hep-ph/9710434; D. Karlen, plenary talk at the *XXIX International Conference of High Energy Physics*, Vancouver, BC, Canada, July 23-29, 1998.

[2] G. Abbiendi *et al.* [OPAL Collaboration], Eur. Phys. J. **C8** (1999) 191; R. Barate *et al.* [ALEPH Collaboration], Phys. Lett. **B453** (1999) 107; P. Abreu *et al.* [DELPHI Collaboration], Phys. Lett. **B456** (1999) 310; M. Acciarri *et al.* [L3 Collaboration], Phys. Lett. **B436** (1998) 437.

[3] B. Abbott *et al.* [D0 Collaboration], Phys. Rev. **D60** (1999) 072002.

[4] See, for instance: *Physics and Technology of the Next Linear Collider: A Report submitted to Snowmass'96 by the NLC Zeroth-Order Design Group and the NLC Physics Working Group*, preprint BNL 52-5-2, FERMILAB-PUB-96/112, LBNL-PUB-5425, SLAC-Report-485, UCRL-ID-124160, UC-414, June 1996; P. Méry, M. Perrottet, and F.M. Renard, Z. Phys. **C38** (1988) 579; A. Barroso and L. Bento, Phys. Rev. **D38** (1988) 2742; F. Boudjema *et al.*, in *Proceedings of e^+e^- Collisions at 500 GeV: The Physics Potential*, edited by P. Zerwas (DESY Report No. 92-123A, B, Hamburg, Germany, 1992), p. 717; U. Baur and E.L. Berger, Phys. Rev. **D47** (1993) 4889.

[5] For a review, see H. Georgi, *Weak Interactions and Modern Particle Theory* (Benjamim/Cummings, Menlo Park, 1984); J.F. Donoghue, E. Golowich and B.R. Holstein, *Dynamics of the Standard Model* (Cambridge University Press, 1992).

[6] K. Hagiwara, S. Ishihara, R. Szalapski and D. Zeppenfeld, Phys. Lett. **B283** (1992) 353; *idem*, Phys. Rev. **D48** (1993) 2182; K. Hagiwara, T. Hatsukano, S. Ishihara and R. Szalapski, Nucl. Phys. **B496** (1997) 66.

[7] C. Arzt, M.B. Einhorn and J. Wudka, Nucl. Phys. **B433** (1995) 41.

[8] K. Hagiwara, R. Szalapski and D. Zeppenfeld, Phys. Lett. **B318** (1993) 155.

[9] K. Hagiwara and M.L. Stong, Z. Phys. **62** (1994) 99; B. Grzadowski and J. Wudka, Phys. Lett. **B364** (1995) 49; G.J. Gounaris, F.M. Renard and N.D. Vlachos, Nucl. Phys. **B459** (1996) 51; W. Killian, M. Krämer and P.M. Zerwas, Phys. Lett. **B381** (1996) 243.

[10] S.M. Lietti, S.F. Novaes, and R. Rosenfeld, Phys. Rev. **D54** (1996) 3266; F. de Campos, S.M. Lietti, S.F. Novaes, and R. Rosenfeld, Phys. Lett. **B389** (1996) 93.

[11] S.M. Lietti and S.F. Novaes, Phys. Lett. **B416** (1998) 441.

[12] G.J. Gounaris, J. Layssac, and F.M. Renard, Z. Phys. **69** (1996) 505; G.J. Gounaris and F.M. Renard, Z. Phys. **69** (1996) 513.

[13] F. de Campos, M.C. Gonzalez–Garcia, and S.F. Novaes, Phys. Rev. Lett. **79** (1997) 5210.

[14] J. Ellis, M.K. Gaillard, and D.V. Nanopoulos, Nucl. Phys. **B106** (1976) 292; A.I. Vainshtein, M.B. Voloshin, V.I. Zakharov, and M.S. Shifman, Sov. J. Nucl. Phys. **30**(1979) 711.

[15] L. Bergstrom and G. Hulth, Nucl. Phys. **B259** (1985) 137; A. Barroso, J. Pulido, J.C. Romão, Nucl. Phys. **B267** (1986) 509.

[16] M.C. Gonzalez-Garcia, Int. J. Mod. Phys. **A14** (1999) 3121, and references therein.

[17] S. Dawson, Nucl. Phys. **B249** (1985) 42; R.P. Kauffman, Phys. Rev. **D41** (1990) 3343; V.D. Barger and R.J.N. Phillips, *Collider Physics*, Addison-Wesley Publishing Co. (1990).

[18] P.W. Johnson, F.I. Olness, and W.-K. Tung, Phys. Rev. **D36** (1987) 291.
[19] V.M. Budnec, I.F. Ginzburg, G.V. Meledin, and V.G. Serbo, Phys. Reports **15C** (1975) 181; See also, S. Brodsky, T. Kinoshita, and H. Terazawa, Phys. Rev. **D4** (1971) 1532.
[20] H. Murayama, I. Watanabe and K. Hagiwara, KEK report 91–11 (1992), unpublished.
[21] T. Stelzer and W.F. Long, Comput. Phys. Commun. **81** (1994) 357.
[22] G.P. Lepage, J. Comp. Phys. **27** (1978) 192.

FIGURES

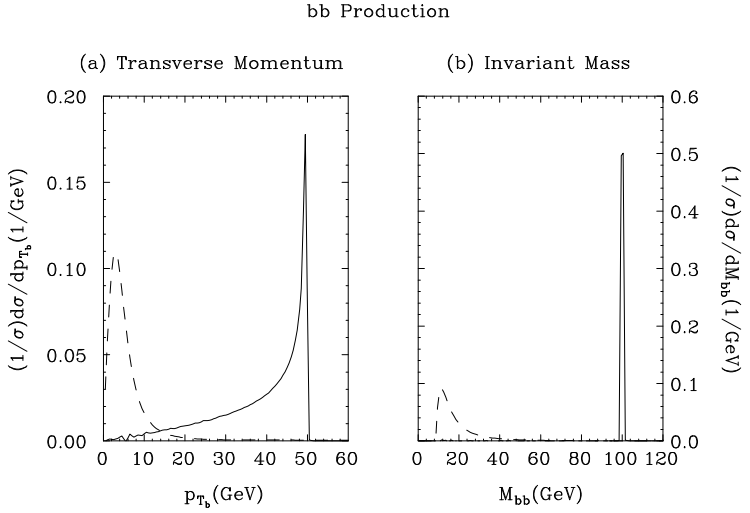

FIG. 1. (a) Transverse momentum distribution of the quark bottom and (b) Invariant mass distribution of the $b\bar{b}$ final state particles at NLC with $\sqrt{s_0} = 500$ GeV and a Higgs boson mass of 100 GeV. The total background is drawn in dashed lines while the full lines are the signal for an anomalous Higgs production via photon fusion ($f_{all} = 30$ TeV^{-2}).

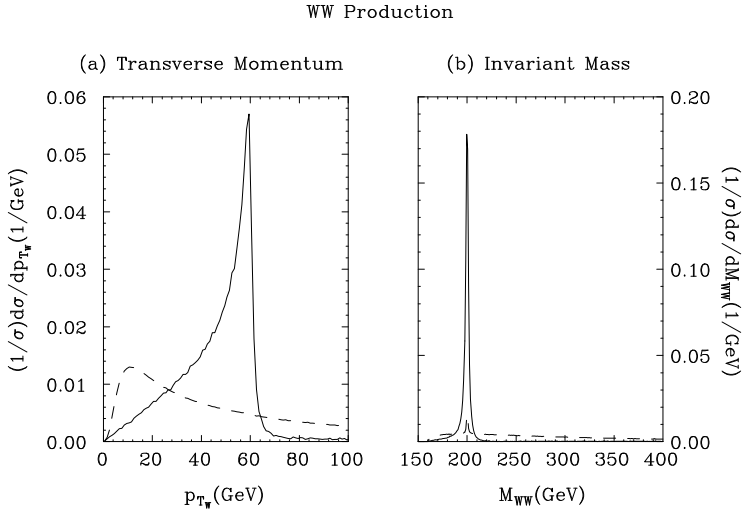

FIG. 2. (a) Transverse momentum distribution of W^+ and (b) Invariant mass distribution of the W^+W^- final state particles at NLC with $\sqrt{s_0} = 1$ TeV and a Higgs boson mass of 200 GeV. The total background is drawn in dashed lines while the full lines are the signal for an anomalous Higgs production via photon fusion ($f_{all} = 30$ TeV^{-2}).

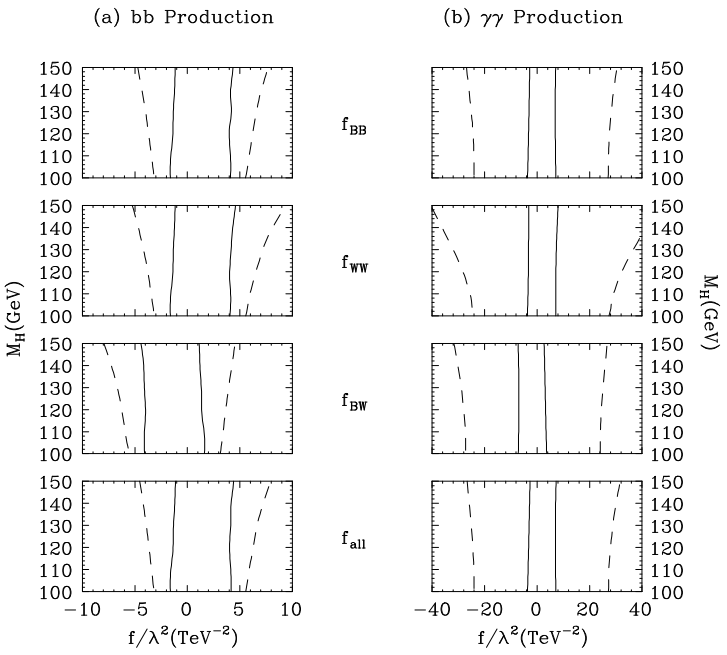

FIG. 3. 95% CL allowed values (inside the lines) of the coefficients f_{BB}, f_{WW}, f_{BW}, and f_{all}, in TeV^{-2}, for: (a) $b\bar{b}$ production and (b) $\gamma\gamma$ production via photon fusion at NLC with $\sqrt{s} = 500$ GeV and $\mathcal{L} = 50$ fb^{-1}, for a Higgs boson mass in the range $100 \leq m_H \leq 150$ GeV. Dashed (full) lines are the limits obtained when a cut in the transverse momentum (invariant mass) distribution is used (see text).

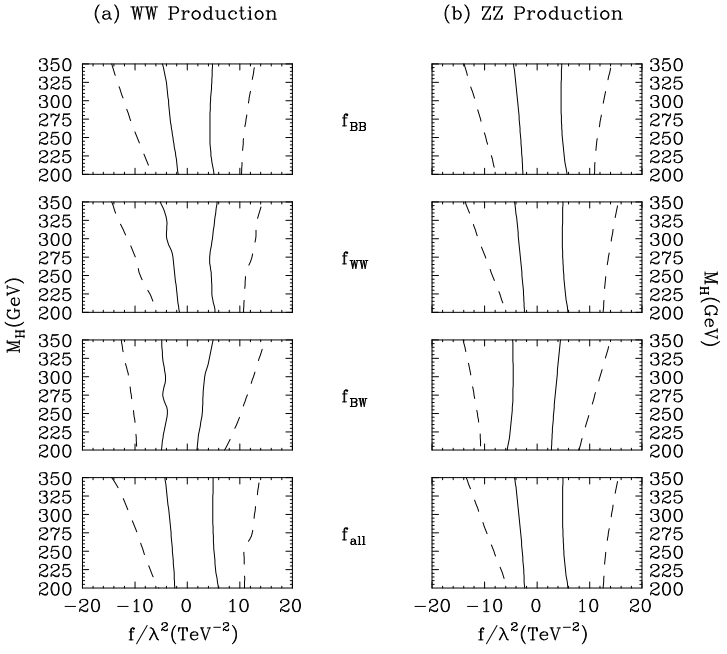

FIG. 4. 95% CL allowed values (inside the lines) of the coefficients f_{BB}, f_{WW}, f_{BW}, and f_{all}, in TeV^{-2}, for: (a) W^+W^- production and (b) ZZ production via photon fusion at NLC with $\sqrt{s_0} = 1$ TeV and $\mathcal{L} = 100$ fb^{-1}, for a Higgs boson mass in the range $200 \leq m_H \leq 350$ GeV. Dashed (full) lines are the limits obtained when a cut in the transverse momentum (invariant mass) distribution is used (see text).

TABLES

Cross Section (fb)	Without Cuts	Transverse Momentum Cut	Invariant Mass Cut
Background ($e^+e^- \to b\bar{b}$)	381	10.9	0
Background ($\gamma\gamma \to b\bar{b}$)	783	6.8	1.7
Background ($W^+W^- \to b\bar{b}$)	9.0	6.2	3.1
Background ($ZZ \to b\bar{b}$)	0.36	0.16	0.13
Signal ($\gamma\gamma \to H \to b\bar{b}$)	66.4	57.6	66.4
Significance	11	66	168

TABLE I. Background and Signal ($f_{all} = 30$ TeV^{-2} and $M_H = 100$ GeV) cross sections (in fb) for the $b\bar{b}$ final state at NLC with a center of mass energy of 500 GeV. The Significance is given by the fraction $\left(\frac{\text{Number of Signal events}}{\sqrt{\text{Number of Background events}}}\right)$ for $\mathcal{L} = 50$ fb^{-1} and e_f=64% overall detection efficiency. The Transverse Momentum Cut is $25 < P_{T_{b,\bar{b}}}(GeV) < (P_{T_{ano}} + 5)$ while the Invariant Mass Cut is $(M_H - 5) < M^{inv}_{b\bar{b}}(GeV) < (M_H + 5)$.

Cross Section (fb)	$P_{T_{\gamma_1,\gamma_2}} > 25$ GeV	Transverse Momentum Cut	Invariant Mass Cut
Background ($e^+e^- \to \gamma\gamma$)	2981	942	0
Background ($\gamma\gamma \to \gamma\gamma$)	$< 8 \times 10^{-5}$	$< 8 \times 10^{-5}$	$< 8 \times 10^{-5}$
Background ($W^+W^- \to \gamma\gamma$)	$< 3 \times 10^{-2}$	$< 2 \times 10^{-2}$	$< 5 \times 10^{-3}$
Background ($ZZ \to \gamma\gamma$)	$< 9 \times 10^{-5}$	$< 9 \times 10^{-5}$	$< 9 \times 10^{-5}$
Signal ($\gamma\gamma \to H \to \gamma\gamma$)	14.7	12.7	14.7
Significance	1.5	2.3	>1200

TABLE II. Background and Signal ($f_{all} = 30$ TeV^{-2} and $M_H = 100$ GeV) cross sections (in fb) for the $\gamma\gamma$ final state at NLC with a center of mass energy of 500 GeV. The Significance is given by the fraction $\left(\frac{\text{Number of Signal events}}{\sqrt{\text{Number of Background events}}}\right)$ for $\mathcal{L} = 50$ fb^{-1} and e_f=64% overall detection efficiency. The Transverse Momentum Cut is $25 < P_{T_{\gamma_1,\gamma_2}}(GeV) < (P_{T_{ano}} + 5)$ while the Invariant Mass Cut is $(M_H - 5) < M^{inv}_{\gamma\gamma}(GeV) < (M_H + 5)$.

Cross Section (fb)	Without Cuts	Transverse Momentum Cut	Invariant Mass Cut
Background ($e^+e^- \to WW$)	2655	633	0
Background ($\gamma\gamma \to WW$)	196	87	9.8
Background ($W^+W^- \to WW$)	5.4	3.4	2.5
Background ($ZZ \to WW$)	0.42	0.32	0.27
Signal ($\gamma\gamma \to H \to W^+W^-$)	36.3	33.8	31.9
Significance	6	11	81

TABLE III. Background and Signal ($f_{all} = 30$ TeV^{-2} and $M_H = 200$ GeV) cross sections (in fb) for the W^+W^- final state at NLC with a center of mass energy of 1 TeV. The Significance is given by the fraction $\left(\frac{\text{Number of Signal events}}{\sqrt{\text{Number of Background events}}}\right)$ for $\mathcal{L} = 100$ fb^{-1} and e_f=80% overall detection efficiency. The Transverse Momentum Cut is $25 < P_{T_{W^+,W^-}}(GeV) < (P_{T_{ano}}+5)$ while the Invariant Mass Cut is $(M_H - 5) < M^{inv}_{W^+W^-}(GeV) < (M_H + 5)$.

Cross Section (fb)	Without Cuts	Transverse Momentum Cut	Invariant Mass Cut
B($e^+e^- \to ZZ$)	147	21.2	0
B($\gamma\gamma \to ZZ$)	0.06	0.05	0.05
B($W^+W^- \to ZZ$)	1.58	0.88	0.92
B($ZZ \to ZZ$)	0.10	0.08	0.09
S($\gamma\gamma \to H \to ZZ$)	6.9	4.6	5.2
Significance ($S/\sqrt{B}$)	5	9	45

TABLE IV. Background and Signal ($f_{all} = 30$ TeV^{-2} and $M_H = 200$ GeV) cross sections (in fb) for the ZZ final state at NLC with a center of mass energy of 1 TeV. The Significance is given by the fraction $\left(\frac{\text{Number of Signal events}}{\sqrt{\text{Number of Background events}}}\right)$ for $\mathcal{L} = 100$ fb^{-1} and e_f=80% overall detection efficiency. The Transverse Momentum Cut is $25 < P_{T_{Z_1,Z_2}}(GeV) < (P_{T_{ano}} + 5)$ while the Invariant Mass Cut is $(M_H - 5) < M^{inv}_{ZZ}(GeV) < (M_H + 5)$.

bb Production

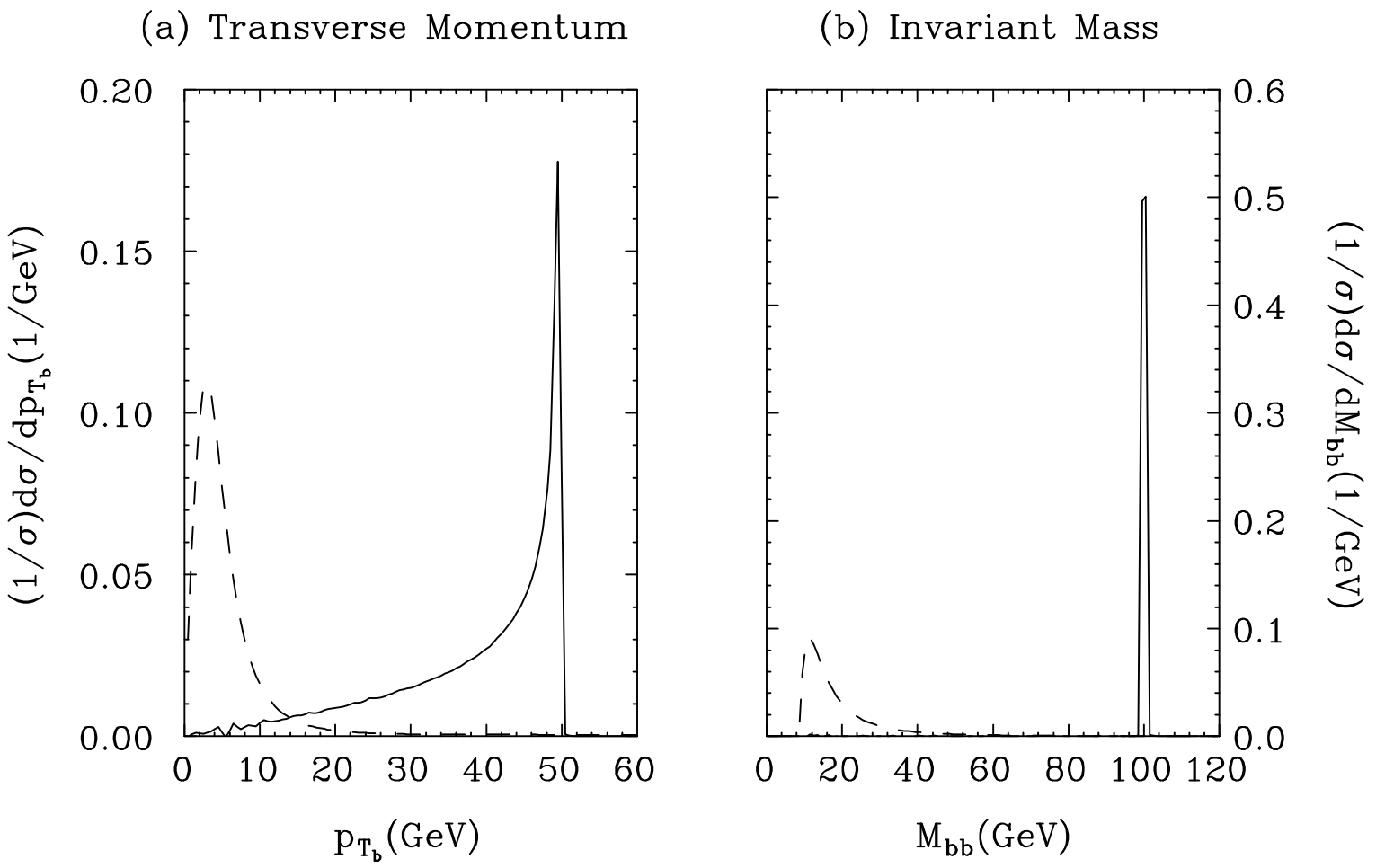

WW Production

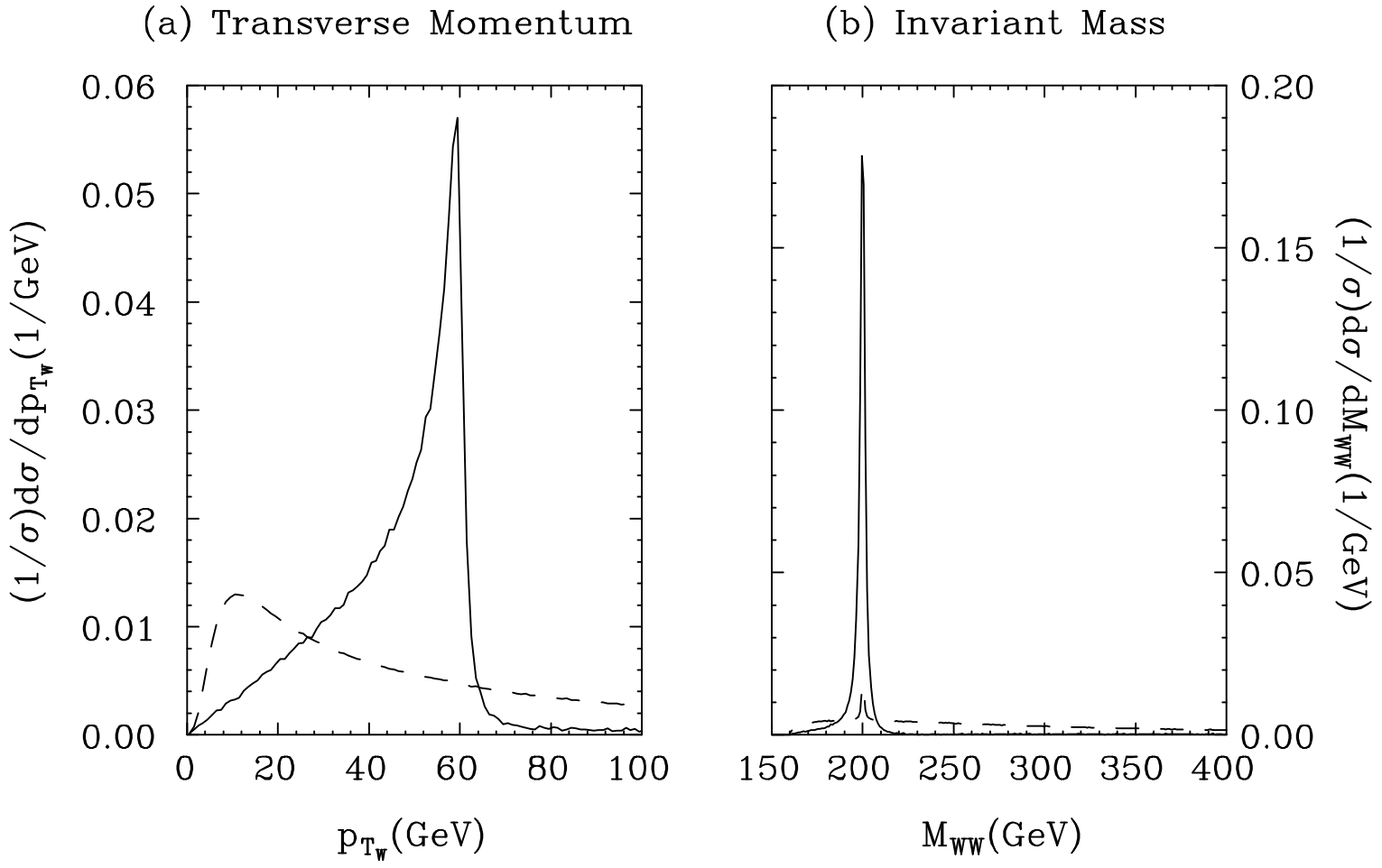

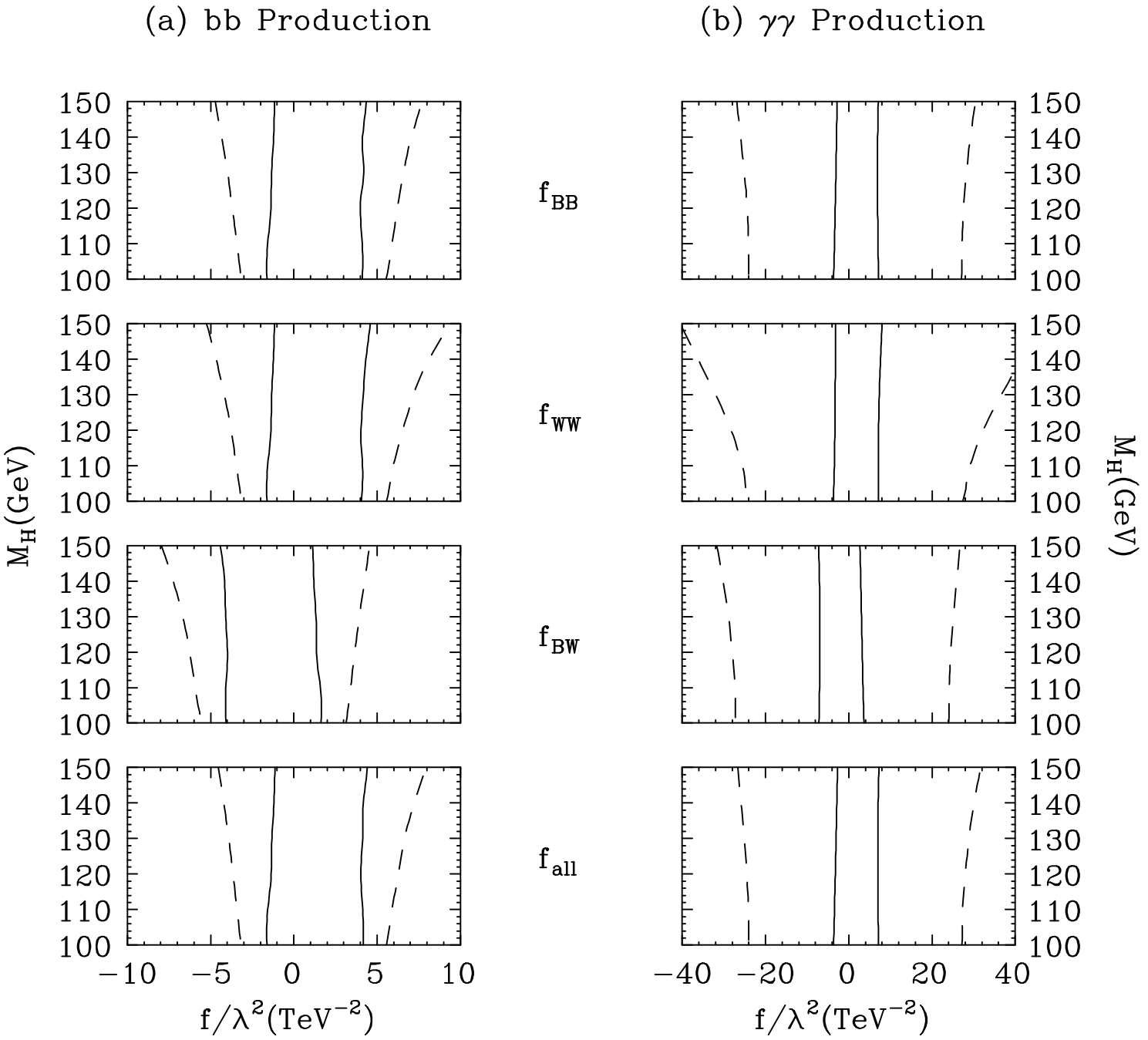
(a) bb Production
(b) γγ Production
f_{BB}
f_{WW}
f_{BW}
f_{all}
M_H(GeV)
f/λ^2(TeV^{-2})
150
140
130
120
110
100
−10
−5
0
5
10
−40
−20
0
20
40

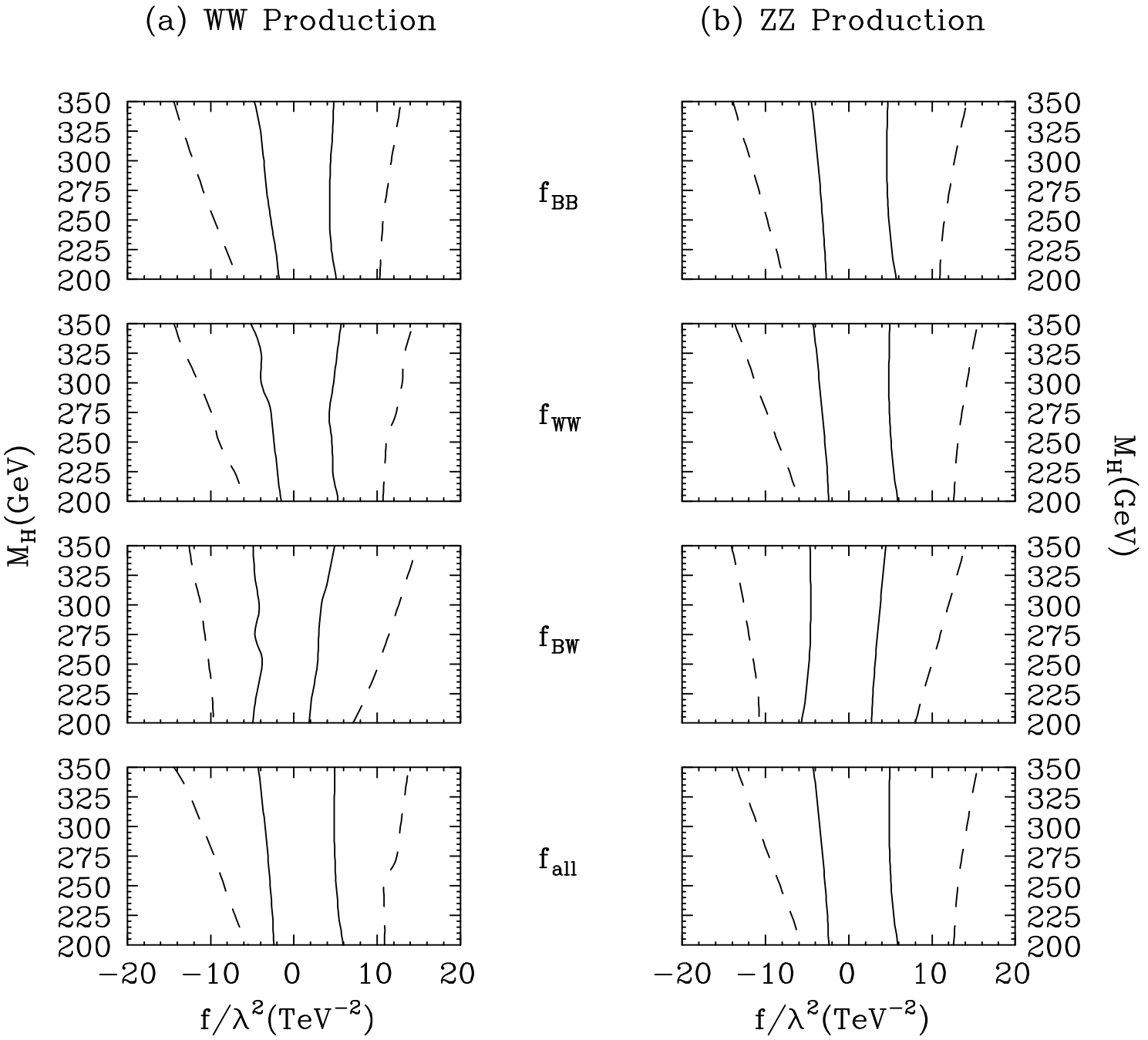
(a) WW Production
(b) ZZ Production
f_{BB}
f_{WW}
f_{BW}
f_{all}
M_H(GeV)
M_H(GeV)
350
325
300
275
250
225
200
−20
−10
0
10
20
f/λ^2(TeV^{-2})
f/λ^2(TeV^{-2})